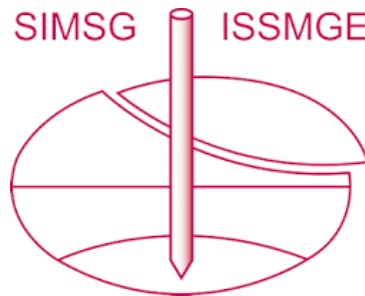


INTERNATIONAL SOCIETY FOR SOIL MECHANICS AND GEOTECHNICAL ENGINEERING



This paper was downloaded from the Online Library of the International Society for Soil Mechanics and Geotechnical Engineering (ISSMGE). The library is available here:

<https://www.issmge.org/publications/online-library>

This is an open-access database that archives thousands of papers published under the Auspices of the ISSMGE and maintained by the Innovation and Development Committee of ISSMGE.

The paper was published in the proceedings of the 7th International Conference on Earthquake Geotechnical Engineering and was edited by Francesco Silvestri, Nicola Moraci and Susanna Antonielli. The conference was held in Rome, Italy, 17 - 20 June 2019.

Field and laboratory assessment of liquefaction potential of crushable volcanic soils

R.P. Orense, M.S. Asadi, M.B. Asadi & M.J. Pender
University of Auckland, Auckland, New Zealand

M.E. Stringer
University of Canterbury, Christchurch, New Zealand

ABSTRACT: Pumice-rich soils originating from volcanic eruptions are deposited in various parts of the world, such as in the central part of North Island, NZ. Since they are often encountered in engineering projects, their geotechnical characterisation is very important. Due to the highly crushable nature of pumice sands, there are concerns on the applicability of current empirical correlations, derived primarily from hard-grained sands, to pumice-rich soils. To understand their liquefaction characteristics, undisturbed soil samples were obtained from various pumice-rich sites in North Island using diverse sampling techniques. The samples were tested in the laboratory using cyclic triaxial apparatus and bender elements. At the same time, various field tests, such as CPT and V_s profiling, were conducted at the same sampling sites. The results clearly showed that crushable volcanic soils do not fit existing frameworks for liquefaction assessment and alternate methods are necessary to characterise them.

1 INTRODUCTION

Soil liquefaction, as a consequence of earthquake shaking, has been one of the main geohazards associated with damages to infrastructure worldwide. For example, the 2010-2011 Canterbury earthquake sequence has demonstrated the impact of soil liquefaction to the built environment (e.g., Cubrinovski and Orense, 2010; Orense et al. 2011; Cubrinovski et al. 2012; Orense et al. 2012a). Consequently, understanding the geotechnical characteristics and seismic behaviour of various local soils is important when designing earthquake-resistant structures.

Pumice sand is a type of volcanic soil that originates within pyroclastic deposits of explosive volcanic events and can be found in numerous locations around the world. For example, pumice-rich deposits are present in the central part of the North Island of New Zealand, in particular, within the Bay of Plenty and Waikato Regions. Currently, they exist mainly as sand layers in river valleys and flood plains as well as coarse gravel deposits in hilly areas. As a consequence of infrastructure development in these regions, these deposits are frequently encountered in engineering projects; hence, the evaluation of their engineering properties is a matter of considerable geotechnical interest.

Pumice sand is characterised by the vesicular make-up of its particles, i.e. the matrix of air-filled chambers some of which are interconnected and open to the surface (called surface voids) while others appear to be isolated inside the particles (called interior voids). As a result, the particles are light weight, highly crushable and compressible, with very rough and angular surfaces. They are very fragile, especially when compared to more “normal” hard-grained sands, such as quartz sand. Because of these special features, soils containing pumice sands are problematic in terms of their geotechnical characterisation. Practising engineers are often faced with questions as to whether current empirical methods for sands, derived primarily from hard-grained (quartz) sands, are also applicable to pumice-rich sands.

This paper presents preliminary results of an on-going extensive investigation being conducted by the authors to characterise the dynamic and liquefaction characteristics of pumice-rich deposits in the central part of North Island. Target sites were first identified and high-quality undisturbed soil samples were obtained using Gel-push and Dames & Moore samplers, as well as conventional push tubes. The samples, both in their undisturbed and reconstituted states, were subjected to undrained cyclic triaxial tests in the laboratory to determine their liquefaction behaviour. At the same time, various in-situ tests, such as cone penetration tests, shear wave velocity profiling and screw driving sounding, were performed at the sites where the samples were obtained. Correlations were then established between the liquefaction resistances obtained from the laboratory-based cyclic tests and those empirically derived from the field data. The results obtained can assist practising engineers on how to deal with pumice-rich soils in the region.

2 CHARACTERISTICS OF PUMICE PARTICLES IN THE REGION

In order to understand the characteristics of the pumice-rich soils investigated in this research, the geology of the Waikato Basin, from which most of the the samples were obtained, is discussed. Next, the properties of the particles are presented, together with their mineralogy and particle characteristics.

2.1 *Geology of Waikato Basin*

Pumice sands were deposited in the Waikato Basin as a consequence of volcanic eruptions within the Taupo Volcanic Zone (TVZ), a north-northeast trending belt of Quaternary volcanism extending for > 300 km across the central North Island (Ewart et al. 1968; Leonard et al. 2010), as indicated in Figure 1. It includes a number of active volcanic vents and has history of major eruptions over the past 1.6 Ma. The air-borne waves of red-hot volcanic debris from these eruptions, which included pumice particles, were lifted into the atmosphere and reached beyond Hamilton City. In addition, the pumice-rich pyroclastic flows generated enormous dust clouds that covered a large area with fine pumice particles (McCraw 2011). After the eruptions, a thick layer of pumice, together with other sediments, formed natural dams, which blocked the outlet of Lake Taupo and parts of the valley of the Waikato River. Subsequently, the dams were overtopped and gave way, washing away all the debris on the choked beds and eroded the riverbanks (Manville et al. 2007). The floodwaters covered large areas with a few meters of mudflow (i.e. the debris of the eruption which included pumice particles). After the flood subsided, the pumice-rich debris were left in the river valley and when the river cut new channels through the muddy, pumice-rich debris, layers of pumice-rich deposits were left on the low terrace of the Waikato River (McCraw 2011). These events



Figure 1. Regional map showing the geographic location of the Taupo Volcanic Zone (TVZ) (after www.sciencelearn.org.nz).

blanketed the region with air-fall and water-rafted pumice deposits that now characterise the geology of the Waikato and Bay of Plenty regions.

2.2 Locations of sampling/testing sites

The target sites where both field testing and soil sampling were conducted in this research are shown in Figure 2. Within the Waikato Basin, four sites were in Hamilton, and one each near the towns of Huntly and Rangiriri; while in Bay of Plenty region, one site was in Whakatane and another in Edgecumbe. At these sites, undisturbed samples were obtained, either by Gel-push sampler (GP-S and GP-Tr; refer to Mori and Sakai (2016) for details), Dames and Moore (DM) sampler, conventional push tubes (PT) or block sampling (see Figure 3). Depths of sampling were chosen based on layer descriptions in the borehole logs. Some of the materials (HAM-1, HAM-2, HUN-1 and RAN-1 sites) were taken from road construction sites where excavations were on-going at the time of sampling. Various field tests were conducted in Whakatane (WHA-1 site), Edgecumbe (EDG-1 site), and in Hamilton (HAM-3 and HAM-4 sites).

In addition, for the purpose of comparison, two other materials were used in the research. One was the commercially-available pure pumice sand. Pumice-rich deposits were quarried at sites in Mercer (about 18 km north of Rangiriri town, along the Waikato River) and the pumice particles were centrifugally separated from other constituents so that the samples consisted of essentially pumice particles. The other material was Toyoura sand, which is known as a hard-grained, sub-angular material and commonly used in Japan.

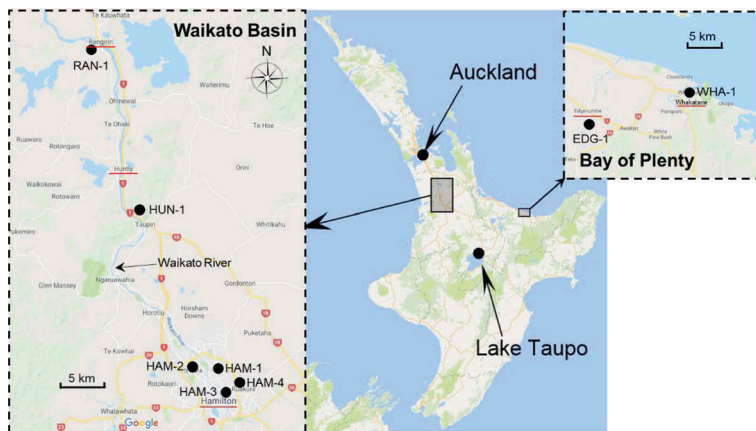


Figure 2. Locations of sampling/testing sites.

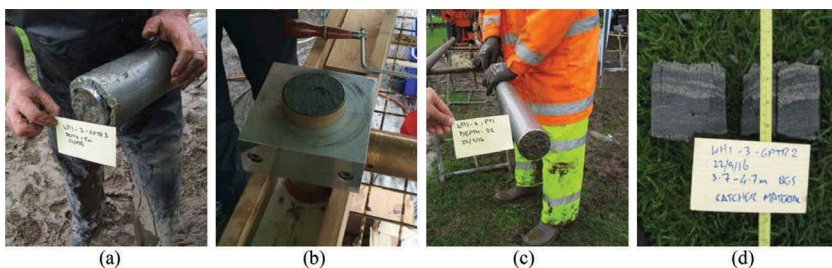


Figure 3. Undisturbed sampling at WHA-1 site: (a) using Gel-push sampler; (b) using Dames & Moore sampler; (c) using push tube; (d) condition of one of the samples.

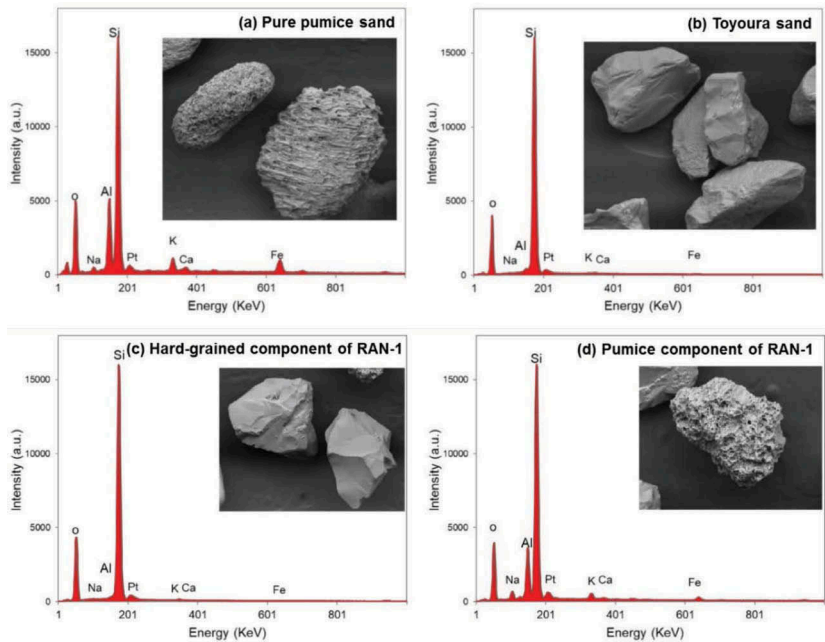


Figure 4. ESEM image and EDS analysis of: (a) pure pumice sand; (b) Toyoura sand; (c) hard-grained component of HAM-1 sand; and (d) pumice component of RAN-1 sand (from Asadi MS et al. 2019).

The index properties and particle size distribution curves of the materials are reported elsewhere (e.g. Asadi MB et al. 2018, 2019; Asadi MS et al. 2017, 2018, 2019; Stringer et al. 2018; 2019).

2.3 Mineralogy of pumice sands

To understand the mineralogy of the various components of the pumice-rich sands from different locations and to compare them with those of pure pumice sand and Toyoura sand, several series of environmental scanning electron microscope (ESEM) imaging accompanied by energy dispersive spectroscopy (EDS) analysis were performed on the materials. Figures 4(a) and 4(b) illustrate the ESEM images and the EDS analysis results for pure pumice sand and Toyoura sand, respectively. As indicated in the figures, the dominant elements in pure pumice sand are silicon, aluminum and oxygen while in Toyoura sand, the dominant elements are only silicon and oxygen. As a representative of the pumice-rich sands, the same set of images for RAN-1 samples are shown in Figures 4(c) and 4(d), corresponding to the hard-grained components and pumice particle components, respectively. As clearly seen in these figures, the hard-grained particles of pumice-rich sand have similar mineralogical composition to Toyoura sand while its pumice particles have similar composition to pure pumice sand. Similar observations were reported by Asadi MS et al. (2019) for the other sites in the Waikato Basin. These images confirmed that the pumice particles present in the pumice-rich sands of the basin are quite similar; i.e. they have similar mineralogy to the pure pumice sand, also sourced from nearby locality.

2.4 Particle shape and crushability

Figures 4(a) and 4(d) indicate that pumice sands have a very unique appearance and are easily distinguishable from the more familiar normal sand particles, as shown in Figures 4(b) and 4(c), specifically with their very irregular surface texture with a lot of surface voids. Asadi MS et al. (2018) investigated the particle shapes of some of the pumice-rich sands obtained and the

Table 1 . Particle shape indices of the sands investigated (from Asadi MB et al. 2018).

Source/Material	Roundness coefficient, R_c	Aspect Ratio, A_r	Angular coefficient, A_c
HAM-1	1.75	1.83	0.52
HAM-2	1.71	1.91	0.50
RAN-1	1.85	1.99	0.56
Toyouira sand	1.26	1.48	0.18
Pure pumice sand*	1.58	1.60	0.45

* as reported by Kikkawa et al. (2013).

particle shape indices are summarised in Table 1. The particle shape indices indicated in the table are the roundness coefficient, R_c , aspect ratio, A_r , and angular coefficient, A_c . These parameters, initially used by Kikkawa et al. (2013) to describe the 2D particle morphology of pure pumice sands, indicate important features of soil particles; for example, $R_c = 1$ shows that the soil particle is circular, and when it exceeds unity the shape changes to ellipsoidal. Furthermore, as the value of $A_r > 1$, the soil particles tend to be more elongated, while higher value of A_c indicates that the soil particle is more angular in shape. The values indicated for each source are the average of > 50 sand particle images analysed. As indicated in the table, the pumice-rich sands are very angular and they tend to be more elongated compared to Toyoura sand.

Also, single particle crushing tests on pure pumice particles showed that their mode of crushing is characterised by gradual breakage followed by a large drop in load when the particle core is crushed; this was different from the observation on hard-grained sand which involved splitting of the particle into 2-3 blocks at the maximum load (Orense et al. 2013a). Moreover, plotting the relation between single particle crushing strength and the initial height of the particle, it was noted that there was a general trend of decreasing strength with increase in particle size, similar to those reported in the literature for silica sand; however, the particle crushing strength of pumice was one order of magnitude less, showing their highly crushable nature.

3 UNDRAINED CYCLIC BEHAVIOUR OF PUMICE-RICH SANDS

Several series of undrained cyclic triaxial tests were performed on both reconstituted and undisturbed pumice-rich specimens obtained at the target sites, as well as on pure pumice sand and Toyoura sand. Some of the results obtained have been reported elsewhere (Orense et al. 2012b, c, d; Orense & Pender 2013, 2015; Asadi MS et al. 2018; Stringer et al. 2019). The following sections highlight the difference in the undrained response between pumice-rich sands and hard-grained (quartz) sands as well as between undisturbed and reconstituted pumice-rich sands.

3.1 Reconstituted pumice-rich sand and Toyoura sand

In order to highlight the difference in the undrained cyclic response of sand containing crushable pumice components with that of hard-grained sand, undrained cyclic triaxial tests were performed on reconstituted specimens to investigate the effect of particle characteristics and crushability on the undrained cyclic behaviour of pumiceous sandy materials. Typical results for medium dense ($D_r=50\%$) pumice-rich sands, in terms of the development of double amplitude axial strain, ε_{DA} , and excess pore water pressure ratio, r_u , with the number of cycles, N , normalised by the number of cycles required to obtain $\varepsilon_{DA}=5\%$, for different cyclic stress ratios ($CSR = \sigma'_d/2\sigma'_c$) are shown in Figure 5. Here, σ'_d is the deviator stress and σ'_c is the initial effective confining pressure..

From the figure, Toyoura sand shows gradual build-up of excess pore water pressure during the early stage of cyclic loading accompanied by negligible strain development; however, the rate of strain development increases dramatically as soon as the specimen reaches r_u

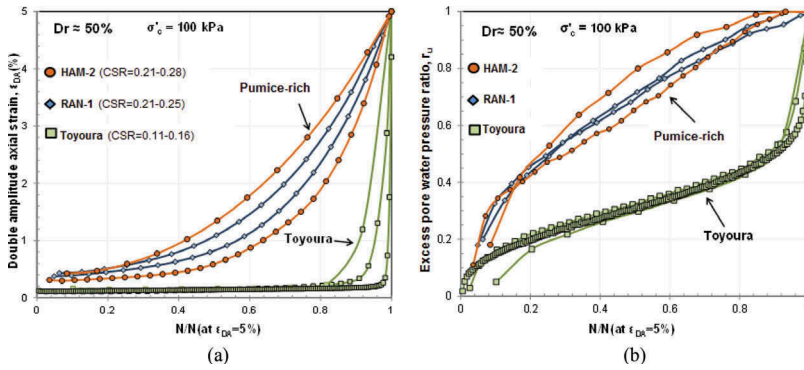


Figure 5. Comparison of undrained cyclic behaviour of medium-dense ($D_r \approx 50\%$) pumice-rich sands and Toyoura sand under different levels of CSR in terms of: (a) double amplitude axial strain; and (b) excess pore water pressure ratio (after Asadi MS et al. 2018).

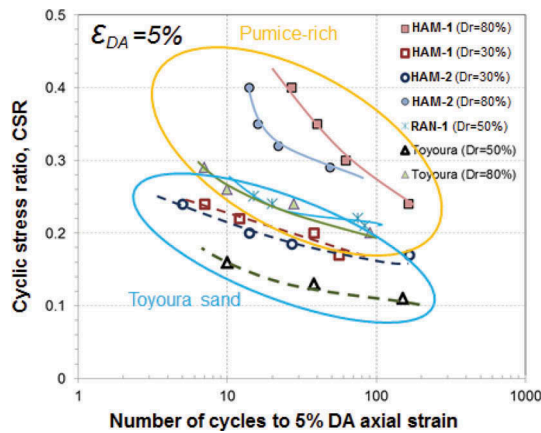


Figure 6. Comparison of liquefaction resistance curves of reconstituted pumice-rich sands and Toyoura sand (Asadi MS et al. 2018).

$\approx 0.5-0.6$. However, the response observed for pumice-rich sand is different; pumice-rich sand specimens undergo significant deformation from the start of cyclic loading accompanied by high r_u development. In the subsequent loading cycles, the axial strain continues to increase at almost linear trend to reach $\epsilon_{DA}=5\%$, while the rate of change of r_u decreases. Essentially similar trend was observed for dense ($D_r=80\%$) specimens. As Asadi MS et al. (2018) pointed out, pumice-rich specimens showed very contractive behaviour during the initial cycle of loading because of the occurrence of particle crushing. However, under high r_u , the behaviour turned very dilative, conceivably because the initial particle crushing and subsequent particle rearrangement, which accompanies the application of the succeeding cycles of loading, lead to a gradual formation of more stable soil skeleton inside the specimen.

The liquefaction resistance curves for some of the materials tested are shown in Figure 6, relating the number of cycles required to attain $\epsilon_{DA}=5\%$ for the specified CSR . As depicted in the figure, the liquefaction resistance of reconstituted pumice-rich sands increases with increasing relative density. It is noteworthy that pumice-rich sands are more resistant to liquefaction compared to Toyoura sand, partly due to the high angularity of the pumice sand components. Since pumice particles have very irregular and angular surface texture, particle crushing causes the contact surface of the particles to increase. While the soil particles crushed and rearranged under the application of initial cyclic loading, the fine crushed materials developed bonds between the particles which provide a higher interlocking effect on the soil samples.

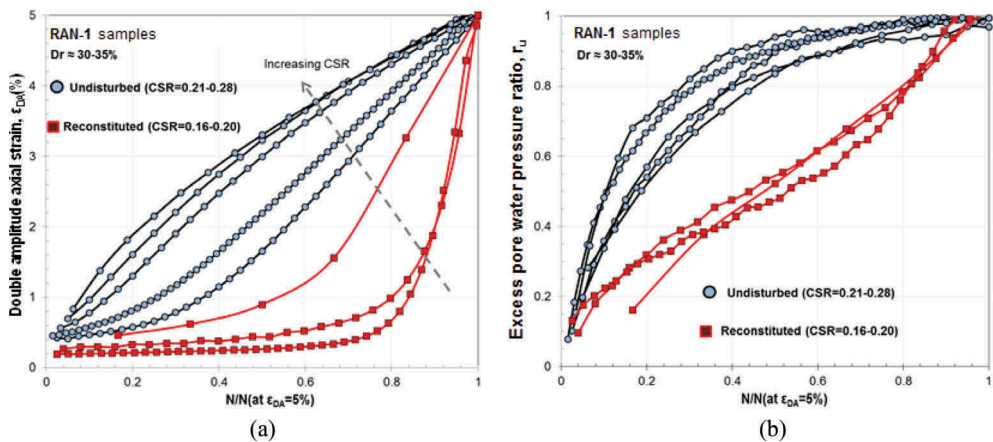


Figure 7. Comparison of undrained cyclic response of undisturbed and reconstituted RAN-1 sand under different levels of CSR : (a) double-amplitude axial strain; (b) excess pore water pressure ratio plotted against normalised number of cycles.

3.2 Undisturbed vs reconstituted pumice-rich samples

Similarly, several series of undrained cyclic triaxial tests were performed on undisturbed pumice-rich sands. To illustrate the influence of soil fabric and structure, the test results on undisturbed pumice-rich sand were compared with those of similar materials reconstituted to the same relative density. Note that due to the different liquefaction resistances of the undisturbed and reconstituted samples, the range of CSR applied to the specimens was different; thus, it was not possible to compare their behaviour under the same CSR . The results shown in Figure 7 are from RAN-1 specimens that underwent liquefaction (reached $\varepsilon_{DA} = 5\%$) after a similar number of cycles.

Based on Figure 7, it is observed that as a result of increase in the CSR , both sets of specimens underwent greater initial deformation. The r_u responses of undisturbed and reconstituted specimens were significantly different. For instance, during the first quarter to the first third of cyclic loading ($N/N_{\varepsilon_{DA}=5\%} \approx 0.25-0.35$), the r_u of undisturbed specimens increased significantly, reaching up to 0.8; this was followed by a gradual increase during subsequent cycles to an $r_u > 0.95$. In contrast, for reconstituted specimens $r_u = 0.1-0.15$ was generated inside the specimens as a result of the first cycle of loading, followed by a gradual increase in r_u . The specimens reached $r_u=0.80$ when the normalised number of cycles was almost 0.8, and initial liquefaction ($r_u=1$) occurred just before ε_{DA} reached 5%. For undisturbed specimens, the rate of increase in strain was almost unaffected by changes in r_u and under $r_u > 0.8$, the specimens were capable of being subjected to significant cyclic loading without undergoing large deformation. In contrast, the reconstituted specimens started to deform faster when $r_u = 0.8$ was reached.

An important feature of the undrained cyclic behaviour of the undisturbed soil samples is that, despite the higher initial compressibility, the specimens show more stable behaviour under high excess pore water pressure. That is, at low mean effective stress (near liquefaction state), a very steady deformation occurred with cyclic loading. This behaviour means that contact is maintained in the particle network, evidence of a stable granular structure.

Figure 8 compares the liquefaction resistance of undisturbed and reconstituted pumice-rich sand specimens from HUN-1 site ($D_r=30-35\%$). It can be seen that the undisturbed specimen is more resistant to liquefaction than the reconstituted one; e.g., the liquefaction resistance of undisturbed sand is about 1.6 times higher than those of reconstituted sand. Moreover, the undisturbed specimens exhibit steeper liquefaction resistance curve. These differences highlight the contribution of the soil fabric, structure and stress history on the liquefaction resistance as the effects of these parameters were erased during the preparation of reconstituted specimens.

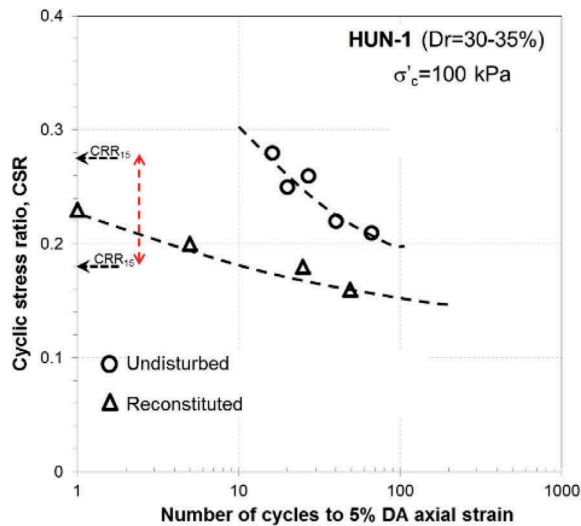


Figure 8. Comparison between liquefaction resistance curves of undisturbed and reconstituted pumice-rich HUN-1 sands.

3.3 Comparison with pumiceous soils found in other parts of the world

Due to the $M_w=7.7$ El Salvador earthquake in 2001, an estimated 200,000 m³ of soil slid along the steep northern flank of the Bálsamo Ridge, which traveled an abnormally long distance of about 700 m into the Las Colinas neighborhood of SantaTecla and covered many houses, burying more than 500 people (Orense et al. 2002); The slide materials involved pyroclastic deposits, i.e., pumiceous sand layers. Subsequent soil sampling and laboratory tests (JSCE 2001) showed that the saturated reconstituted pumice samples ($D_r=50\%$) had CRR_{20} (cyclic shear stress ratio required to reach $\varepsilon_{DA}=5\%$ in 20 cycles) as low as 0.22.

Gratchev and Towhata (2010) investigated the Aratozawa landslide, which extended about 1200 m long and 800 m wide, triggered by the $M_w=6.9$ 2008 Iwate-Miyagi Nairiku earthquake (Japan). Based on their field investigation, the material exposed at the scarp of the slides was identified mostly as heavily weathered pumice. The results of undrained cyclic triaxial tests showed $CRR_{20}=0.20$ for reconstituted specimens and 0.25 for undisturbed specimens.

Similarly, following the $M_w=6-7$ earthquake sequence which rocked Kumamoto Prefecture (Japan) in April 2016, many geo-disasters were reported in the Mount Aso Caldera, such as the large-scale flow-type slope failure referred to as the Takanodai landslide (Chiaro et al. 2017). Early field observations suggested that the key soil layer which caused the slope failure was the orange-coloured pumice soil deposit. Based on undrained cyclic triaxial tests on the Aso pumice soil, Sumartini et al. (2018) reported a CRR_{20} of 0.29 for reconstituted specimens and 0.48 for undisturbed specimens. Similarly, Chiaro et al. (2018) reported a $CRR_{20}=0.21$ for reconstituted samples ($\rho_d=0.58-0.63$ g/cm³) from undrained cyclic torsional shear tests.

Thus, the NZ pumice soils investigated herein appear to have more or less similar liquefaction resistance, in both reconstituted and undisturbed states, as those reported for pumice sands found in Japan and El Salvador. However, it would be best to compare these pumiceous soils also in terms of particle shape characteristics, mineralogy and development of pore water pressure and strain with number of cycles, as well as in terms of degree of packing, degree of weathering and pumice contents.

4 FIELD TESTING AT PUMICE-RICH SITES

Previous research at the University of Auckland showed that the penetration resistance (q_c) values obtained from cone penetration tests (CPT) on pure pumice sand were only marginally



Figure 9. Field testing conducted in Whakatane (WHA-1 site): (a) CPT and sCPT; and (b) SDS test.

influenced by the density of the material. The reason for this behaviour is possibly because the stresses imposed by the penetrometer are so severe that particle breakage forms a new material and that its properties are nearly independent of the initial state of the sand (Wesley et al. 1999). Thus, conventional relationships between the q_c value and relative density, which in turn is correlated with liquefaction resistance, appear to be not valid for these soils.

A previous research by the authors showed that penetration-based approaches, such as cone penetration tests and seismic dilatometer tests, underestimated the value of liquefaction resistance of the pumice deposits, confirming that any procedure where the liquefaction resistance is correlated with density will not work on pumice-rich deposits (Orense et al. 2012b; Orense and Pender 2013, 2015). The same research showed that empirical method based on shear wave velocity seemed to produce good correlation with liquefaction resistance of pumiceous soils. Admittedly, the above conclusions were obtained from limited number of test data and such conclusions have not been well validated. With many consultants and practitioners constantly asking for advice on how to evaluate the liquefaction susceptibility of pumice deposits, there is a need to clarify and address this issue.

Case histories of occurrence/non-occurrence of liquefaction during earthquakes have provided the basis for many of the currently available empirical methods for evaluating liquefaction potential (Youd et al., 2001; Idriss & Boulanger 2008). Field test results, such as CPT and shear wave velocity profiling, have been used by many researchers to explain the observed performance at many sites in Christchurch following the 2010-2011 Canterbury Earthquake Sequence (e.g., Orense et al. 2014; Wotherspoon et al. 2015; Lees et al. 2015). By estimating the liquefaction resistance of the soil (through field-based parameters) and comparing it with the shear stress induced by the earthquake (which is related to the peak ground acceleration), the Factor of Safety against Liquefaction (FoS) can be obtained; hence, if the liquefaction resistance is less than the induced cyclic shear stress (i.e. $FoS < 1$), the deposit is deemed to have liquefied.

Within the current research programme, various field tests have been conducted at sites where the high-quality samples were obtained. Field tests including CPT, shear wave velocity profiling, and screw driving sounding have been conducted in the Bay of Plenty Region (WHA-1 and EDG-1 sites in Figure 2), as well as in Hamilton (HAM-3 and HAM-4 sites in Figure 2). Photos showing some of the tests are shown in Figure 9.

In the following sections, the results of recent investigation to evaluate the liquefaction occurrence in pumice-rich deposits due to the 1987 Edgecumbe earthquake are presented.

4.1 Field testing at known liquefaction sites

Two sites where liquefaction had been observed during the 1987 Edgecumbe Earthquake were considered in this research. Test site WHA-1 was located adjacent to the Whakatane Sewage Pump station, while Test EDG-1 was opposite the Edgecumbe substation (refer to Figure 2). Manifestations of soil liquefaction, such as sand boils and ejected materials, have been reported at both sites (Pender & Robertson 1987).

At both sites, borehole sampling, cone penetration test (CPT), seismic cone penetration test (sCPT), and screw driving sounding (SDS) were performed. SDS is a new in-situ method that has recently been developed in Japan, where a rod is drilled into the ground at several loading steps at the same time as the rod is being continuously rotated. Details of this test are reported elsewhere (e.g., Orense et al. 2013b, 2019) The SDS test is fast, the machine is small in size and the implementation is relatively cheap, compared to other in-situ testing methods.

Boreholes from the two tests sites indicate the presence of fine to coarse sand layers intermittently mixed with pumice. At the Whakatane (WHA-1) site, the presence of pumice sands were visible between 0.5-7 m, while at the Edgumbe (EDG-1) site, pumice was mixed with fine to medium sand from 0.5-6.2 m. The ground water table was located at about 2 m from the surface at both sites. Details are provided by Orense et al. (2017). The results of the field tests showed that at WHA-1 site, the cone tip resistance was about $q_c=4$ MPa up to a depth of 5 m and it increased to about $q_c=8$ MPa up to a depth of 10 m. The soil behaviour type (SBT), derived from CPT data, indicated alternating layers of sand and silt mixtures up to a depth of 5 m, and predominantly sand up to a depth of 12 m. The shear wave velocity profile showed V_s ranging from 90-120 m/s up to a depth of 5 m, after which V_s increased with depth, reaching 170 m/s at depth of 11 m. During the SDS test, several parameters were measured every 25 cm; these include torque, load, speed of penetration, depth of penetration and friction on the rod. An important parameter derived was the specific energy of penetration, E_s , representing the sum of the contribution of the torque and applied load for every load step normalised by the volume of penetration (Mirjafari et al. 2016). At WHA-1 site, $E_s < 25$ N.mm/mm³ up to a depth of 10 m, below which stiff layer with $E_s < 50$ N.mm/mm³ existed. At EDG-1 site, q_c was generally < 8 MPa, except at depths of 3.0-3.5 m and > 6.5 m; V_s generally varied between 110-170 m/s. SDS indicated $E_s < 30$ N.mm/mm³, except at depths of 3.0-3.5 m and > 6.5 m. From all tests, a hard layer was apparent at depth of approximately 7 m, where $q_c > 20$ MPa, $V_s > 160$ m/s, and $E_s > 70$ N.mm/mm³; all tests were terminated at this depth. Again, further details are reported by Orense et al. (2017).

4.2 Evaluation of liquefaction triggering

For the purpose of evaluating the liquefaction triggering at both sites during the Edgumbe earthquake, six simplified empirical methods were employed: three CPT-based methods – i.e. those proposed by Boulanger and Idriss (2014), Robertson and Cabal (2012) and Moss et al. (2006); two V_s -based methods – i.e. those proposed by Andrus and Stokoe (2000) and Kayen et al. (2013); and the SDS-based method proposed by Mirjafari et al. (2016). Per the analyses of Mellso (personal communication), the Edgumbe earthquake, with moment magnitude $M_W=6.5$, induced the following peak ground accelerations (PGA): 0.29g in WHA-1 site and 0.53g in EDG-2 site. More details about PGA distribution in the Bay of Plenty region due to the Edgumbe earthquake are discussed by Mellso (2017).

In terms of ground water table (GWT), Pender and Robertson (1987) reported the following: “the earthquake occurred at the end of the summer and after a long period of dry weather. Most of the deposits underlying the Rangitaiki Plains are saturated, with the water table ranging from near surface in the coastal margin, to about 3 m below ground level in the Te Teko area. (In Edgumbe), the top of the soil profile is a layer of about 3 m thickness which is very loose, (and) at the time of the earthquake, the water table was probably towards the bottom of this layer over much of the plains.” Thus, in the analyses, the GWT location was assumed at: 1 m, 2 m and 3 m from the ground surface for WHA-1 site, and 2 m, 3 m and 4 m for EDG-1 site.

Considering the input parameters mentioned above, liquefaction assessment was conducted using the 6 simplified methods. Results for WHA-1 site (with GWT=2 m) and for EDG-1site (with GWT=3 m) are shown in Figures 10 and 11, respectively. In the figures, the depth profile of the cyclic stress ratio (CSR) and cyclic resistance ratio (CRR) are plotted, and the shaded regions represent the pumice-rich zones which are deemed to have liquefied (i.e. $CRR < CSR$).

Based on the results, it is clear that at WHA-1 site, where field testing has been done up to a depth of 11.5 m, all the methods considered would predict liquefaction of pumiceous deposits (between the depth ranging from the location of the water table up to 7 m depth). Similarly, at EDG-1 site, all methods would predict pumice liquefaction between GWT up to 7 m depth.

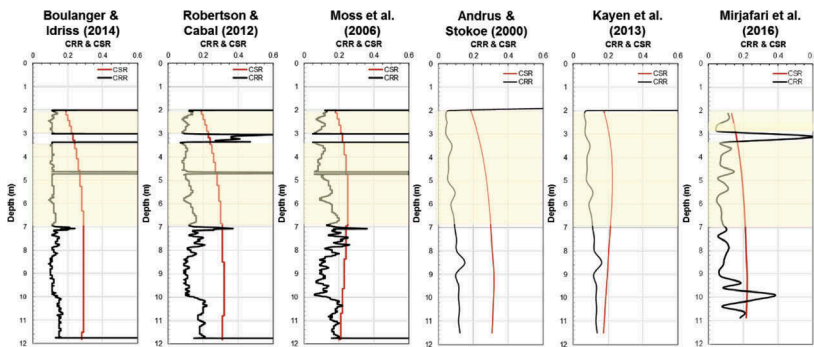


Figure 10. Liquefaction triggering results for WHA-1 site, with GWT=2.0 m.

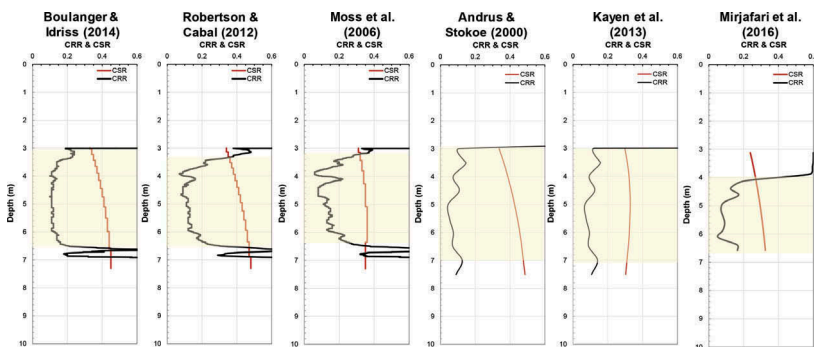


Figure 11. Liquefaction triggering results for EDG-1 site, with GWT=3.0 m.

Similar results were obtained for the other GWT locations. Thus, it would appear that for the sites selected, all empirical methods were able to predict the occurrence of liquefaction of the pumice layers, consistent with the observed manifestation of liquefaction at the sites as reported in the literature. However, based on the results of the analyses, it is observed that for both sites, the calculated $FoS \approx 0.5$; this may be due to things: (1) the CSR induced by the earthquake, manifested by the PGA used, is generally high such that the sites would have liquefied anyway, whether or not pumice sand components are present; and (2) the CRR , estimated using field-based parameters, significantly underestimated the actual liquefaction resistance of the pumice-rich soils. A value of $FoS \approx 0.5$ over a significant depth (> 4 m) indicates severe liquefaction, which is not consistent with the few sand boils reported to have occurred at the sites (i.e., the reported liquefaction would correlate, at best, to FoS just below 1.0); thus, assuming the estimated $PGAs$ are correct, it would appear that the CRR used is substantially underestimated.

Having obtained high-quality samples at sites where the field tests have been performed, the next phase of the research was to attempt to correlate the liquefaction resistance obtained in the laboratory using cyclic triaxial tests and those estimated using field-based parameters.

5 LABORATORY-DERIVED AND FIELD-ESTIMATED LIQUEFACTION RESISTANCE

5.1 Examination of sample quality

Before doing the correlation, the quality of the samples obtained using various sampling techniques was examined using two methods: (a) visual inspection; and (b) comparison of shear

wave velocity in the field and in the laboratory. For this purpose, the quality of the samples obtained at WHA-1 site is discussed below.

5.1.1 Visual observation of samples

Ocular examination of the quality of the samples obtained was first conducted immediately after the sampling, since the overall quality of the samples obtained was, at that state, not affected by the succeeding processes, such as handling, transport and laboratory preparation. In the case of the samples obtained by the Gel-push (GP-S) sampler at depths shallower than 3.5 m ($q_c \approx 2$ MPa), they appear to be in very good condition, with the ends of the samples appearing to be firm, and not showing any visual signs of distress when the core liner was removed from the tool. Once free of the tool, the sample was found to be sliding very easily in the tube, and an attempt to cut the sample into smaller sub samples on site provided further evidence that the sample was visually in very good condition. However, samples taken at deeper depths ($q_c \approx 5$ MPa) were compromised, with the sample deformed in the core liner (Figure 3a). The recovery with the Dames & Moore sampler was good (Figure 3b), though in some cases, the cutting edge at the front of the tubes was dented as a result of hitting gravel-sized pumice particles. Samples obtained by conventional push tube all had very good recovery (Figure 3c); however, when the tubes were removed from the tool, it was apparent that the top of the samples were slurry-like and therefore were considered to have been disturbed. Overall, it appeared that any of the sampling techniques adopted in WHA-1 site resulted in, more or less, good quality specimens. Further details are discussed by Stringer et al. (2018).

5.1.2 Comparison of V_s from field and laboratory

Attempting to assess the true quality of undisturbed specimens remains very difficult, especially in sandy materials, where approaches developed for clayey materials (e.g. $\Delta e/e_0$, as proposed by Andresen & Kolstad 1979) are not appropriate. In sandy materials, a number of researchers have used shear wave velocity (linked to shear stiffness) to compare the small strain behaviour of undisturbed specimens in the laboratory.

Thus, the soil specimens obtained from WHA-1 site were frozen on-site and transported to the laboratories at University of Auckland (UoA) and University of Canterbury (UC). Following the above approach, the shear wave velocity was determined for a number of specimens using bender elements at different effective confining stress levels. Details of bender element testing on pumice-rich samples are discussed by Asadi MB et al. (2018, 2019) and Stringer et al. (2018).

Figure 12 illustrates the quality of the samples obtained by various sampling techniques prior to testing. Again, ocular inspection seems to indicate that most of the samples are of high quality, unaffected by the handling, transport and trimming they were subjected to. Also, it is clear from the figure the difficulties faced in characterising these soils in the field as revealed by the soil structure preserved in the samples. That is, in addition to the layering observed in hard-

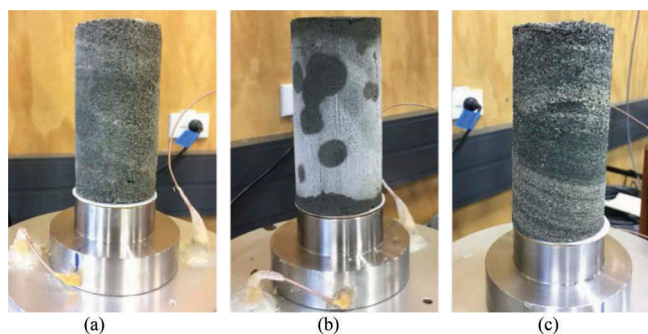


Figure 12. Examples of undisturbed specimens prior to laboratory testing, obtained by: (a) GP-S sampler; (b) DM sampler; and (c) conventional push tube.

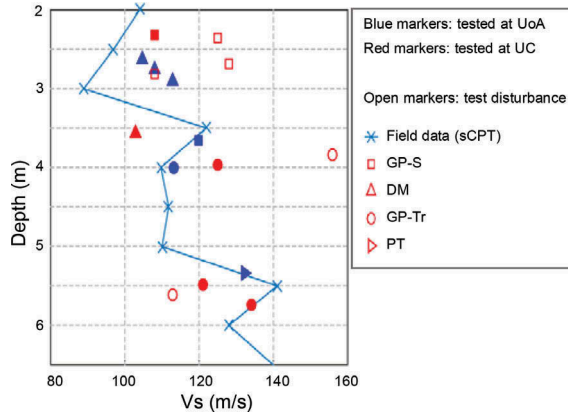


Figure 13. Comparison of field-obtained V_s profile from sCPT and V_s measured from bender elements in the laboratory.

grained materials, the pumice content can vary significantly, from one end of the sample to the other. Within any particular soil unit, the pumice components can also be distributed in either relatively homogeneous manner, or exist in many thin bands. These issues pose additional challenges that need to be considered in understanding their response, and highlight the possible effect of different depositional modes on the behaviour of pumice-rich sandy deposits.

Figure 13 compares the field-obtained shear wave velocity profile from sCPT measurements, and those obtained in the laboratory using bender elements. In the figure, the lab-based V_s data obtained from the two laboratories are indicated, where the open markers indicate the effect of sample disturbance in the laboratory (Stringer et al. 2018). In general, the open markers lie further from the field-measured V_s as compared to tests where there were no known testing problems. The samples that were judged to be “good” lie within $\pm 15\%$ of the field measurements. Obviously, there are many uncertainties associated with the plot, such as: the sensitivity of V_s to the applied effective stress level, the assumed K_0 -value and unit weights of the soil, the accuracy of determining the arrival time in BE testing, and factors associated with field measurement of V_s , among others. While these aspects require further investigation in order to make a definitive conclusion on the quality of specimens based on small strain measurements, the general trend seems to indicate acceptable level of quality of the samples obtained.

5.2 Correlation between laboratory-obtained and field-based CRR

The results of undrained cyclic triaxial tests are typically summarised in the form of liquefaction resistance curve, as discussed earlier. In view of the typical number of significant cycles present in many time histories of accelerations recorded during past earthquakes, it is customary to consider 15 cycles of loading, representing $M_w=7.5$ earthquake, to estimate the liquefaction resistance (or cyclic strength) of the soil; herein, this is referred to as $(CRR)_{triaxial} = (\sigma_d/2\sigma_c)$.

However, the conditions the laboratory specimens were subjected to are different from those in-situ. Hence, in order to estimate the in-situ liquefaction resistance, $(CRR)_{field} = \tau_{cyclic}/\sigma'_v$, corrections need to be applied to the laboratory-obtained values, as follows:

$$\left(\frac{\tau_{max}}{\sigma'_v}\right)_{field} = C_1 \cdot C_2 \cdot C_3 \cdot C_4 \cdot C_5 \cdot (CRR)_{triaxial} \quad (1)$$

$$(CRR)_{field} = \left(\frac{\tau_{cyclic}}{\sigma'_v}\right)_{field} = 0.65 \left(\frac{\tau_{max}}{\sigma'_v}\right)_{field} \quad (2)$$

where, according to Ishihara (1985) and Towhata (2008):

- C_1 – correction due to difference in consolidation stress. $C_1=(1+2K_0)/3$ where $K_0=0.5$ for normally consolidated soils;
- C_2 – correction due to difference in loading condition, where earthquake loading is irregular while laboratory specimens are subjected to sinusoidal waves. $C_2=1/0.65$ or $(=1/0.55-0.70)$;
- C_3 – correction due to sample disturbance. $C_3 > 1$, but not clearly understood yet;
- C_4 – correction due to densification during handling. $C_4 < 1$, but not clearly understood yet;
- C_5 – correction due to loading direction, where earthquake loading is at least two components, E-W and N-S. $C_5=0.80-0.90$.

For normally consolidated soils, $K_0=0.5$, therefore, $C_1=(1+2\times 0.5)/3=0.67$; moreover, $C_3.C_4 \approx 1$ is assumed, since the quality of the samples is unpredictable. By further assuming $C_5=0.90$, it follows that

$$(CRR)_{field} \approx 0.67 \cdot 0.9 \cdot (CRR)_{triaxial} \approx 0.60 \cdot (CRR)_{triaxial} \quad (3)$$

Thus, in liquefaction potential evaluation, the in-situ cyclic resistance ratio can be taken as 60% of the laboratory-derived cyclic resistance.

Using the above procedure, the $CRR_{triaxial}$ corresponding to 15 cycles from all the undrained cyclic triaxial tests conducted to date (with effective confining pressure $\sigma'_c=100$ kPa) are collated and correlated to the field parameter (CPT, V_s or E_s of SDS) measured at the specified depth where the samples were obtained. These are then plotted in the empirical charts, as shown in Figure 14. In the figure, the CPT-based chart is that proposed by Boulanger and Idriss (2014), while the V_s -based chart and SDS-based chart are from the procedure proposed by Kayen et al. (2013) and Mirjafari et al. (2016). Note that all the charts are for clean sands (fines content $FC < 5\%$) and correspond to $M_w=7.5$ earthquake and $\sigma'_v=1$ atm ($=100$ kPa). Also incorporated in the figure are the data points reported by Orense & Pender (2013) based on their previous study; since SDS tests were not conducted then, the penetration energy in SDS ($E_{s,1}$) was estimated from correlation with CPT data, as reported by Orense et al. (2019).

It can be observed from the figure that all the three field-based methods generally underestimate the liquefaction resistance of the pumice-rich deposits. Although the solid lines indicated are for clean sands and the actual samples have some amount of fines (up to $FC=20\%$ maximum), the appropriate curves may shift a bit to the right; however, the change would not be that significant. While penetration-based methods, such as CPT (Figure 14a) and SDS (Figure 14c), are expected to provide underestimation due to particle crushing when the rods penetrate into the pumice-rich layer, even the V_s -based approach (Figure 14b) also underestimated the CRR . This is contrary to the initial finding reported by Orense & Pender (2013), where their observation showed good correlation between lab-derived and V_s -based CRR (derived using the chart proposed by Andrus and Stokoe, 2000). Their contention then was that although the V_s they used was obtained from seismic dilatometer test (sDMT) where the

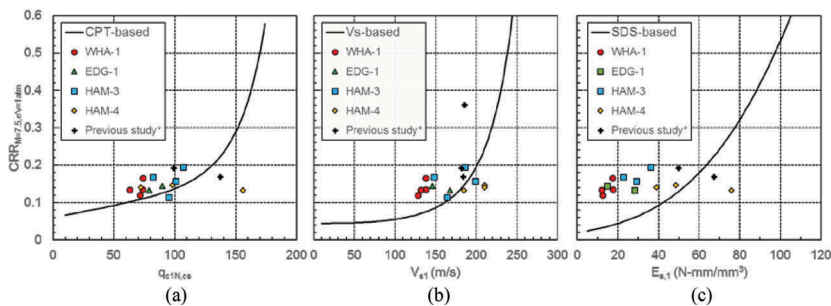


Figure 14. Comparison between lab-obtained and field-based CRR : (a) using CPT; (b) using V_s ; (c) using SDS.

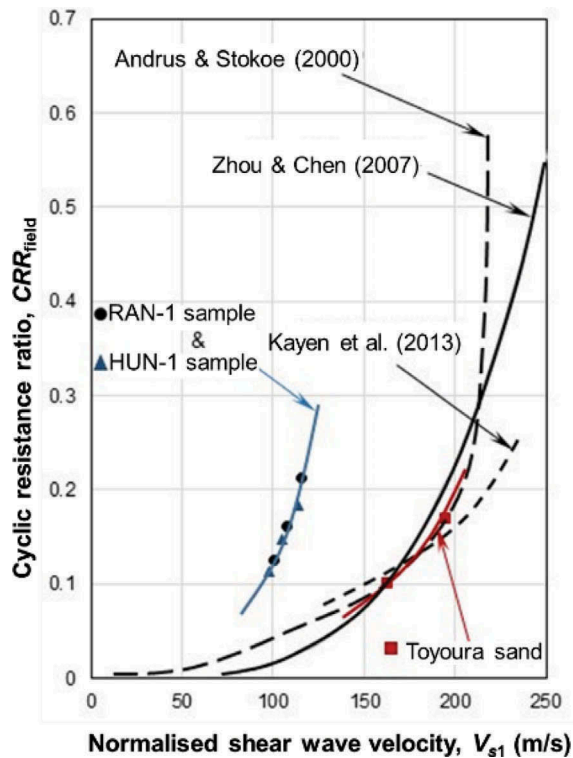


Figure 15. $(CRR)_{field} - V_{s1}$ correlations for the tested pumice-rich materials and comparison with available correlations in literature (modified from Asadi MB et al. 2018).

penetrating rod may have induced particle breakage in the pumice zone adjacent to the rod, the shear waves travelled through the intact grains and not on the crushed ones, and therefore the V_s measured reflected the actual state of the ground. However, with more data obtained in recent testing and sampling at WHA-1, EDG-1, HAM-3 and HAM-4 sites, the present trend seems to indicate otherwise.

To investigate this, a number of cyclic triaxial and bender element tests were performed on two types of reconstituted pumice-rich sands (from HUN-1 and RAN-1 sites), as well as on Toyoura sand, to estimate their CRR and V_s , respectively; details are reported by Asadi MB et al. (2018). The obtained correlations for pumice-rich sands were compared with those derived for Toyoura sand, as well as to other hard-grained sands reported in the literature, and the comparison is shown in Figure 15.

Asadi MB et al. (2018) noted that under similar D_r and σ'_c , pumice-rich sands have considerably lower V_s when compared to that of Toyoura sand due to the presence of crushable, porous and lightweight pumice particles with irregular surface texture. Moreover, under similar D_r and σ'_c , the liquefaction resistance of pumice-rich sands was higher than that of Toyoura sand due to the complex surface texture and the occurrence of particle crushing during cyclic loading, which resulted in more stable soil structure during cyclic shear application. As a result, the $CRR_{field} - V_{s1}$ relations for reconstituted pumice-rich sands plotted considerably to the left side of data for hard-grained sands. Of course, since the tests were performed on reconstituted sands, the effect of soil fabric, structure and stress history on the behaviour of the specimens are not accounted for. However, if these parameters are taken into account, it is expected that both CRR and V_{s1} of pumice-rich sands would increase, and may result in a trend similar to that of reconstituted specimen; in fact, it may not be too different to the data trend shown in Figure 14(b).

Finally, two significant parameters have not been taken into consideration in the above analyses: (1) the amount of pumice particles mixed within the soil matrix of the deposit (i.e., soil samples with significant pumice content would have more crushable particles present, while those with small or negligible pumice content would behave in the same way as hard-grained sands); and (2) the mode of deposition of the pumice components (i.e. whether the pumice components were deposited as ash fall or via fluvial deposition would affect the soil structure, which in turn would affect the liquefaction resistance of the sand. Further investigations are currently being conducted to comprehend these issues.

5.3 *Current state of practice*

Currently, many large engineering projects are being constructed in volcanic areas, especially in the Waikato – Bay of Plenty region, and the “normal” practice is to implement ground improvement measures every time pumice-rich deposits are encountered. However, as the above discussions indicate, the existing empirical correlations being preferred by the local profession, which are based on natural hard-grained sands, would not work for the characterisation of pumice deposits and could mislead engineering assessment.

At this stage of the research, performing laboratory undrained cyclic tests on high-quality undisturbed samples of pumice-rich soils is the best way of characterising these deposits. Thus, in lieu of field testing, laboratory testing is recommended as this would significantly reduce the costs spent in mitigating potentially non-existent liquefaction hazards.

6 CONCLUDING REMARKS

In order to investigate the liquefaction characteristics of pumice-rich deposits in the central part of North Island, NZ, an extensive research programme has been conducted consisting of image analyses, field testing, high-quality sampling and laboratory testing. Target sites for testing and sampling, identified through borehole logs, included sites in the Waikato Basin (Hamilton, Huntly, Rangiriri) and in Bay of Plenty region (Whakatane and Edgumbe). Some of the findings of the research are as follows:

- Environmental scanning electron microscope (ESEM) imaging and energy dispersive spectroscopy (EDS) analysis showed that the pumice sand particles present in pumice-rich soils from the identified target sites are quite similar, indicating they came from identical source (s). These pumice sand components are very crushable (particle strength is one order of magnitude less than normal sands) and have very irregular surface shape and texture due to their vesicularity.
- Such peculiar features of the pumice sand components make pumiceous samples behave differently when subjected to undrained cyclic shear loading, when compared to normal sands. Due to particle crushing and subsequent interlocking, the patterns of development of axial strain and excess pore water pressure during cyclic loading are different, leading to their higher liquefaction resistance.
- High quality undisturbed sampling of pumice-rich sands is possible with techniques currently available in NZ. In particular, based on the experience of the authors, Gel-push sampler seems to provide the best samples from the target sites.
- Comparison of the liquefaction resistances obtained from undisturbed samples using cyclic triaxial tests with those estimated using field parameters (CPT, V_s and SDS) indicate that the latter provides underestimation. Hence, current field-based methods of estimating liquefaction potential derived for normal sands would not work for pumice-rich sands.
- At this stage, performing laboratory undrained cyclic tests on high-quality undisturbed samples of pumice-rich soils is the best way of characterising these deposits.
- Future work should focus on the role of pumice content and deposition mode to better understand their behaviour.

ACKNOWLEDGMENTS

Parts of the results presented in this paper was supported financially by the Natural Hazard Research Platform and by the QuakeCoRE, a New Zealand Tertiary Education Commission-funded Centre. Some of the sampling and testing works have been conducted with the help of S.Y. Mirjafari, N. Papen & J. Melster of the Geomechanics Laboratory, University of Auckland and I. Haycock of McMillan Drilling. Furthermore, the assistance of Tonkin + Taylor Ltd and Opus International Consultants Ltd in facilitating access to some sites and in providing some samples and site details is gratefully acknowledged. The support of Whakatane District Council, AECOM and GNS Science in determining the target test sites is gratefully acknowledged. This is QuakeCoRE publication number 0425.

REFERENCES

- Andresen, A. & Kolstad, P. 1979. The NGI 54 samplers for undisturbed sampling of clays and representative sampling of coarser materials. *Proc. Int. Symposium on Soil Sampling*, Singapore, 13–21.
- Andrus, R.D. & Stokoe, K.H. II. 2000. Liquefaction resistance of soils from shear-wave velocity. *Journal of Geotechnical and Geoenvironmental Engineering, ASCE*, 126(11): 1015–1025.
- Asadi, M.B., Asadi, M.S., Orense, R.P. & Pender, M.J. 2018. Shear wave velocity-based assessment of liquefaction resistance of natural pumiceous sands. *Géotechnique Letters*, 8(4): 1–6.
- Asadi, M.B., Orense, R.P., Asadi, M.B. & Pender, M.J. 2019. Liquefaction assessment of pumiceous sand with shear wave velocity approach. *Proc., 7th Int. Conference on Earthquake Geotechnical Engineering*, Rome, Italy (to appear).
- Asadi, M.S., Asadi, M.B., Orense, R.P. & Pender, M.J. 2017. Undrained cyclic and post-liquefaction behaviour of natural pumiceous soils. *3rd Int. Conf. Performance-based Design in Earthquake Geotech Engg (PBD-III)*, Vancouver, BC, Canada, Paper 334, 7pp.
- Asadi, M.S., Asadi, M.B., Orense, R.P. & Pender, M.J. 2018. Undrained cyclic behavior of reconstituted natural pumiceous sands. *Journal of Geotechnical and Geoenvironmental Engineering, ASCE*, 144 (8):04018045.
- Asadi, M.S., Asadi, M.B., Orense, R.P. & Pender, M.J. 2019. Maximum dry density test to quantify pumice content in natural soils. *Soils & Foundations* (under review).
- Boulanger, R.W. & Idriss, I.M. 2014. CPT and SPT based liquefaction triggering procedures. *Report No. UCIDI/CGM-14/01*, Center for Geotechnical Modeling, University of California, Davis, CA, 134 pp.
- Chiaro G., Alexander G., Brabhaharan P., Massey C., Koseki J., Yamada S. & Aoyagi Y. 2017. Reconnaissance report on geotechnical and geological aspects of the 2016 Kumamoto Earthquake, Japan. *Bulletin of the New Zealand Society for Earthquake Engineering* 50(3): 365–393.
- Chiaro G., Umar, M., Kiyota, T. & Massey C. 2018. The Takanodai landslide, Kumamoto, Japan: insights from post-earthquake field observations, laboratory tests and numerical analyses. *Proc. Geotechnical Earthquake Engineering and Soil Dynamics V (GSP 293)*, Austin Texas, 98–111.
- Cubrinovski, M. & Orense, R.P. 2010. Case history: 2010 Darfield (New Zealand) Earthquake – Impacts of liquefaction and lateral spreading. *ISSMGE Bulletin*, 10pp.
- Cubrinovski, M., Robinson, K., Taylor, M., Hughes, M. & Orense, R. 2012. Lateral spreading and its impacts in urban areas in the 2010-2011 Christchurch earthquake. *NZ Journal of Geology & Geophysics*, 55(3): 255–269.
- Gratchev, I. & Towhata, I. 2010. Geotechnical characteristics of volcanic soil from seismically induced Aratozawa landslide, Japan. *Landslides*, 7:503–510.
- Ewart, A. 1968. The petrography of the central North Island rhyolitic lavas. Part 2 - regional petrography including notes on associated ash-flow pumice deposits. *NZ Journal of Geology & Geophysics*, 11: 478–545.
- Idriss, I.M. & Boulanger, R.W. 2008. Soil liquefaction during earthquakes. *MNO-12*, Earthquake Engineering Research Institute, Oakland, CA.
- Ishihara, K. 1985. Stability of natural deposits during earthquakes. *Proc., 11th Int. Conference on Soil Mechanics & Foundation Engineering*, San Francisco, CA, 1:321–376.
- Japan Society of Civil Engineers, JSCE 2001. *The January 13, 2001 Off the Coast of El Salvador Earthquake*, Tokyo, Japan, 112pp.
- Kayen, R.E., Moss, R.E.S., Thompson, E.M., Seed, R.B., Cetin, K.O., Der Kiureghian, A., Tanaka, Y. & Tokimatsu, K. 2013. Shear-wave velocity-based probabilistic and deterministic assessment of

- seismic soil liquefaction potential. *Journal of Geotechnical and Geoenvironmental Engineering, ASCE*, 139(3): 407–419.
- Kikkawa, N., Orense, R.P. & Pender, M.J. 2013. Observations on microstructure of pumice particles using computed tomography. *Canadian Geotechnical Journal*, 50(11): 1109–1117.
- Lees, J.J., Ballagh, R.H., Orense, R.P. & van Ballegooy, S. 2015. CPT-based analysis of liquefaction and re-liquefaction following the Canterbury earthquake sequence. *Soil Dynamics & Earthquake Engineering*, 79B: 304–314.
- Leonard, G.S., Begg, J.G. & Wilson, C.J.N. 2010. *Geology of the Rotorua Area*. Institute of Geological and Nuclear Sciences 1:250,000 geological map 5. sheet + 102 p. Lower Hutt, New Zealand. GNS Science.
- Manville, V., Hodgson, K. & Nairn, I. 2007. A review of break-out floods from volcanogenic lakes in New Zealand. *NZ Journal of Geology & Geophysics*, 50: 131–150.
- McCraw, J. 2011. The Wandering River: Landforms and geological history of the Hamilton Basin. *Geoscience Soc. NZ Guidebook, No. 16*, Geoscience Society of New Zealand.
- Mellso, N. 2017. Liquefaction Case Histories from the 1987 Edgcumbe Earthquake – Insights from an Extensive CPT dataset, direct push cross hole shear and compression wave velocity (V_sV_p) testing and paleo-liquefaction trenching. *Master Thesis*, University of Auckland, NZ.
- Mirjafari, Y., Orense, R.P. & Suemasa, N. 2016. Soil classification and liquefaction evaluation using Screw Driving Sounding. *Proc., 5th Int. Conference on Geotechnical & Geophysical Site Characterisation*, Gold Coast, Australia, 6pp.
- Mori, K. & Sakai, K. 2016. The GP sampler: a new innovation in core sampling. *Journal of Australian Geomechanics Soc.*, 51(4): 131–166.
- Moss, R.E.S., Seed, R.B., Kayen, R.E., Stewart, J.P., Der Kiureghian, A. & Cetin, K.O. 2006. CPT-based probabilistic and deterministic assessment of in situ seismic soil liquefaction potential. *Journal of Geotechnical and Geoenvironmental Engineering, ASCE*, 132(8): 1032–1051.
- Orense, R.P., Vargas-Monge, W. & Cepeda, J. 2002. Geotechnical aspects of the January 13, 2001 El Salvador earthquake. *Soils and Foundations*, 42(4): 57–68.
- Orense, R.P., Kiyota, T., Yamada, S., Cubrinovski, M., Hosono, Y., Okamura, M. & Yasuda, S. 2011. Comparison of liquefaction features observed during the 2010 and 2011 Canterbury earthquakes. *Seismological Research Letters*, 82(6): 905–918.
- Orense, R.P., Pender, M.J. & Wotherspoon, L.M. 2012a. Analysis of soil liquefaction during the recent Canterbury (New Zealand) earthquakes. *Geotechnical Engineering Journal of SEAGS & AGSSEA*, 43(2): 8–17.
- Orense, R.P., Pender, M.J. & O’Sullivan, A. 2012b. Liquefaction characteristics of pumice sands. *Final Report of EQC Project 10/589*, 131pp.
- Orense, R.P., Hyodo, M. & Kaneko, T. 2012c. Dynamic deformation characteristics of pumice sand. *Proc. NZSEE Annual Technical Conference*, 8pp.
- Orense, R.P., Pender, M.J. & Tai, A. 2012d. Undrained cyclic shear behaviour of pumice sand. *Proc., Australia-NZ Conference on Geomechanics*, Melbourne, 6pp.
- Orense, R.P., Pender, M.J., Hyodo, M. & Nakata, Y. 2013a. Micro-mechanical properties of crushable pumice sands. *Géotechnique Letters*, 3 (Issue April-June): 67–71.
- Orense, R.P. & Pender, M.J. 2013b. Liquefaction characteristics of crushable pumice sand. *Proc. 18th Int. Conference on Soil Mechanics & Geotechnical Engineering*, Paris, 4pp.
- Orense, R.P., Mirjafari, Y. & Suemasa, N. 2013. Geotechnical site characterisation using screw driving sounding method. *Proc. NZ-Japan Workshop Soil Liquefaction during Recent Large-scale Earthquakes*, Auckland, NZ, 11–20.
- Orense, R.P., Hickman, N.A., Hill, B.R. & Pender, M.J. 2014. Spatial evaluation of liquefaction potential in Christchurch in the 2010/2011 Canterbury earthquakes. *Int. Journal of Geotechnical Engineering*, 8(4): 420–425.
- Orense, R.P. & Pender, M.J. 2015. From micro to macro: An investigation of the geomechanical behaviour of pumice sand. *Keynote Lecture, Int. Workshop Volcanic Rocks & Soils*, Isles of Ischia, Italy, 45–62.
- Orense R.P., Wotherspoon, L.M., Pender, M.J., van Ballegooy, S. & Cubrinovski, M. 2017. Applicability of field-based methods for evaluating liquefaction potential of pumiceous deposits. *Proc. 20th NZGS Geotechnical Symposium*, Napier, 8pp.
- Orense, R.P., Mirjafari, Y. & Suemasa, N. 2019. Screw driving sounding: a new test for field characterization. *Geotechnical Research* (in press).
- Pender, M.J. & Robertson, T.W. (eds). 1987. Edgcumbe Earthquake: Reconnaissance Report. *Bulletin of the New Zealand Society for Earthquake Engineering*, 20(3): 201–249.

- Robertson, P.K. & Cabal, K.L. 2012. *Guide to Cone Penetration Testing for Geotechnical Engineering*, 5th edition, Gregg Drilling & Testing, 131pp.
- Stringer, M.E., Orense, R.P., Pender, M.J. & Haycock, I. 2018. Undisturbed sampling of pumiceous deposits in New Zealand. *Proc. Geotechnical Earthquake Engineering and Soil Dynamics V (GSP 293)*, Austin Texas, 394–403.
- Stringer, M.E., Asadi, M.B., Orense, R.P., Asadi, M.S. & Pender, M.J. 2019. Cyclic behavior of undisturbed samples from pumice-rich soils. *Proc., 7th Int. Conference on Earthquake Geotechnical Engineering*, Rome, Italy (to appear).
- Sumartini, W.O., Hazarika, H. Kokusho, T. & Ishibashi, S. 2018. Volcanic cohesive soil behaviour under static and cyclic loading. *Proc., 20th SEAGC - 3rd AGSSEA Conference*, Jakarta, Indonesia.
- Towhata, I. 2008. *Geotechnical Earthquake Engineering*, Springer Science & Business Media, Berlin.
- Wesley, L.D., Meyer, V.M., Pronjoto, S., Pender, M.J., Larkin, T.J. & Duske, G.C. 1999. Engineering properties of pumice sand. *Proc. 8th Australia-NZ Conference on Geomechanics*, Hobart, 2: 901–908.
- Wotherspoon, L.M., Orense, R.P., Green, R.A., Bradley, B.A., Cox, B.R. & Wood, C.M. 2015. Assessment of liquefaction evaluation procedures and damage potential frameworks at Christchurch strong motion stations. *Soil Dynamics & Earthquake Engineering*, 79B: 335–346.
- Youd, T.L., Idriss, I.M., Andrus, R.D., Arango, I., Castro, G., Christian, J.T., Dobry, R., Finn, W.D.L., Harder, L.F., Hynes, M.E., Ishihara, K., Koester, J.P., Liao, S.S.C., Marcuson III W.F., Martin, G. R., Mitchell, J.K., Moriwaki, Y., Power, M.S., Robertson, P.K., Seed, R.B. & Stokoe II K.H. 2001. Liquefaction resistance of soils: summary report from the 1996 NCEER and 1998 NCEER/NSF workshops on evaluation of liquefaction resistance of soils. *Journal of Geotechnical and Geoenvironmental Engineering, ASCE*, 127(10): 817–833.
- Zhou, Y. G. & Chen, Y. M. 2007. Laboratory investigation on assessing liquefaction resistance of sandy soils by shear wave velocity. *Journal of Geotechnical and Geoenvironmental Engineering, ASCE*, 133(8): 959–972.